

The CONNIE experiment with Skipper CCDs

Irina Nasteva

Universidade Federal do Rio de Janeiro (UFRJ)
on behalf of the CONNIE collaboration

Magnificent CEvNS workshop
Munich, Germany, 22 March 2023



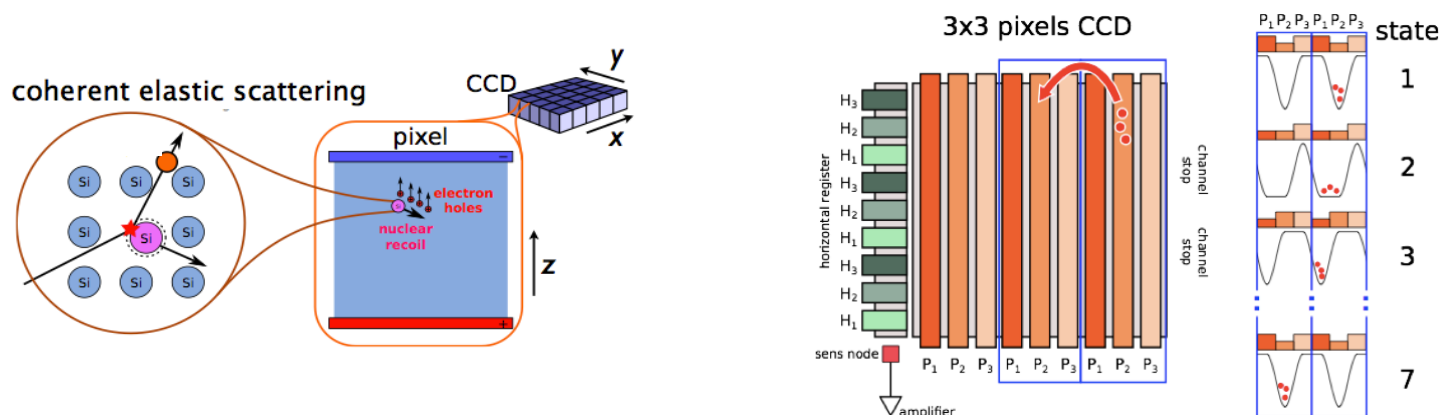


The CONNIE experiment



- Coherent Neutrino-Nucleus Interaction Experiment (CONNIE).
- The main goal is to detect coherent elastic scattering of reactor antineutrinos off silicon nuclei and place limits on physics Beyond the Standard Model.
- The detectors are thick (675 μm) scientific CCDs made from high resistivity silicon.
 - Charges are collected in potential wells and read out sequentially.
 - Low noise ($\sim 2\text{ e}^-$) and low dark current ($\sim 3\text{ e}^-/\text{pix}/\text{day}$)*.
 - Low-energy detection threshold ($\sim 50\text{ eV}$)*.

* with standard CCDs



Centro Atómico Bariloche, Universidad de Buenos Aires, Universidad del Sur / CONICET, Centro Brasileiro de Pesquisas Físicas, Universidade Federal do Rio de Janeiro, CEFET – Angra, Universidade Federal do ABC, Instituto Tecnológico de Aeronáutica, Universidad Nacional Autónoma de México, Universidad Nacional de Asunción, University of Zurich, Fermilab



The CONNIE experiment

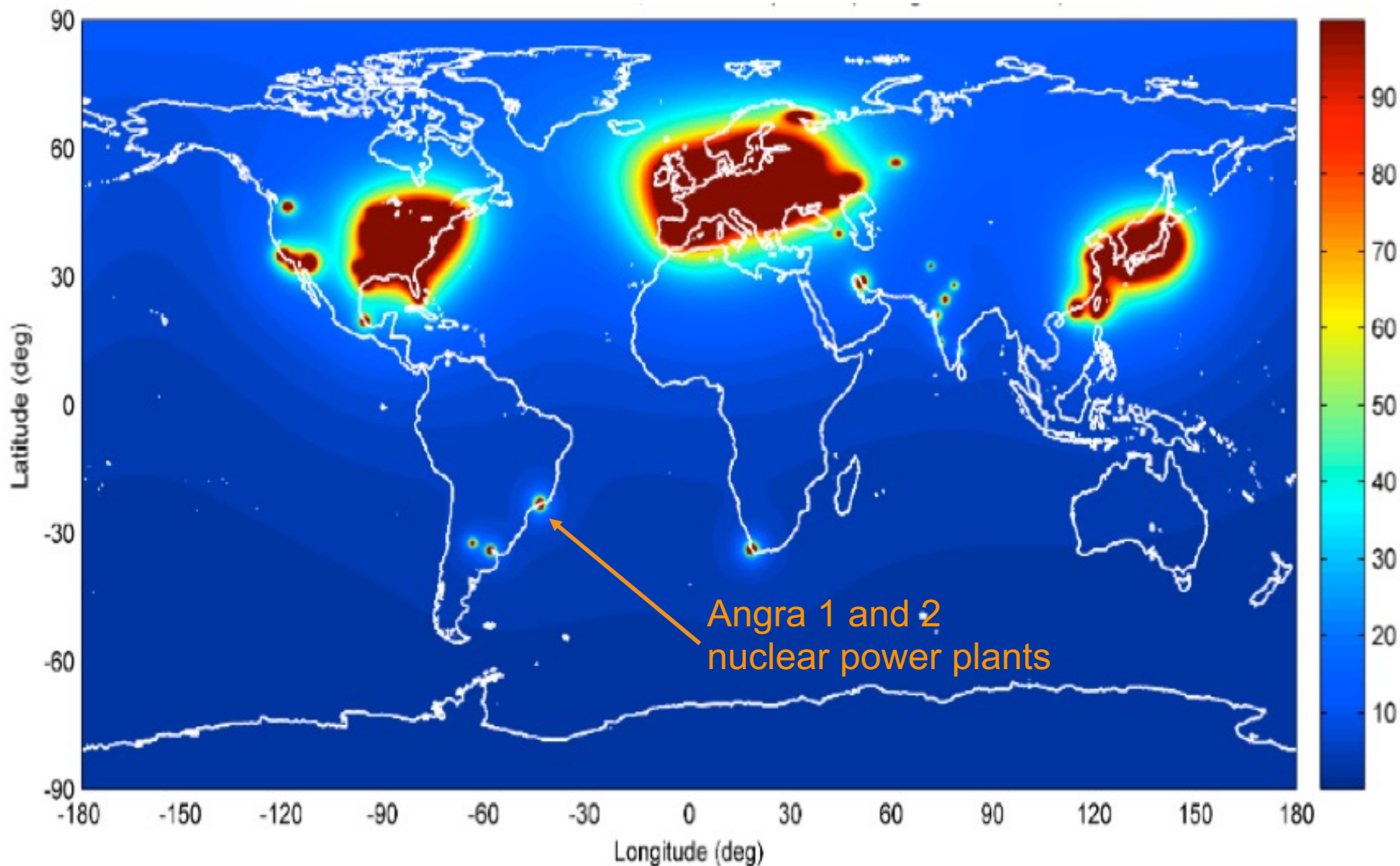


- CONNIE is located next to the Angra 2 reactor at the Almirante Álvaro Alberto nuclear power plant, near Rio de Janeiro, Brazil.



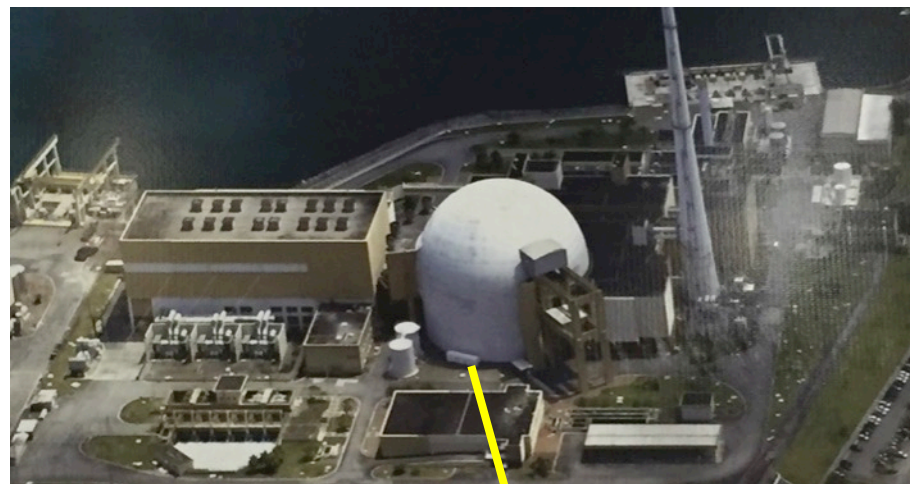


Reactor antineutrinos



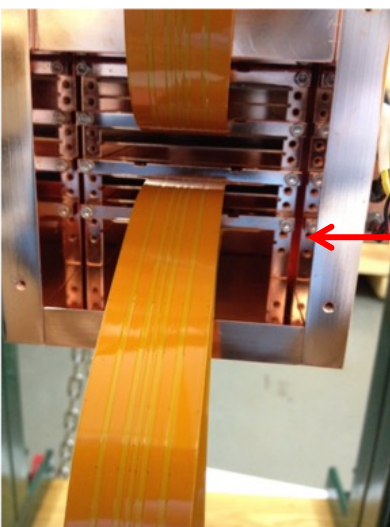
The CONNIE experiment

- At around 30 m from the nucleus of the 3.95 GW_{th} Angra 2 reactor.
- Shared lab with the Neutrinos Angra experiment.
- Antineutrino source with flux of $7.8 \times 10^{12} \bar{\nu} \text{s}^{-1} \text{cm}^{-2}$ at the detector position.





The CONNIE detector



CCDs in
copper box

ViB readout board
(signal transport)

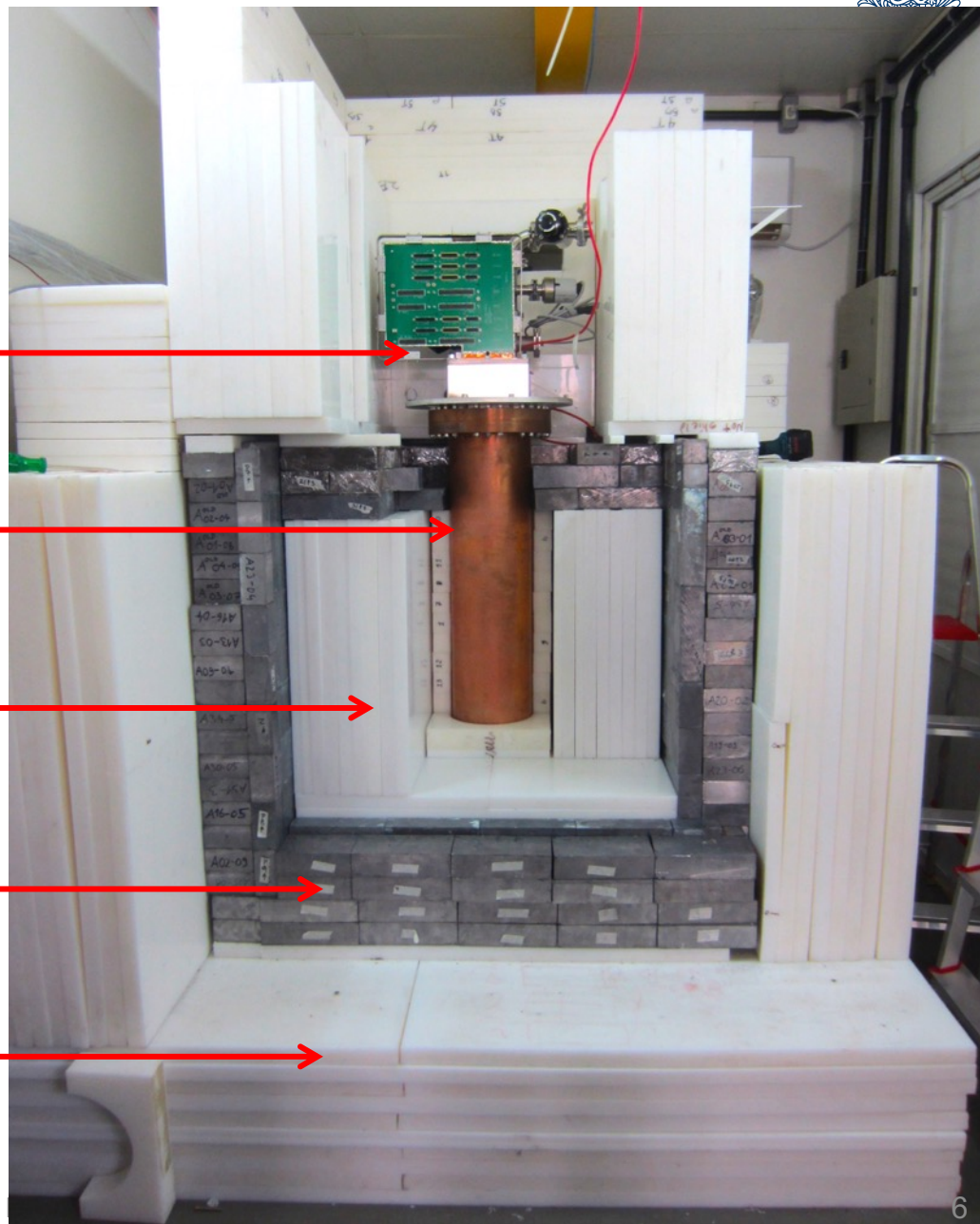
Engineering run:
JINST 11 (2016) P07024

Dewar
(vacuum)

Inner Polyethylene – 30 cm
(neutrons)

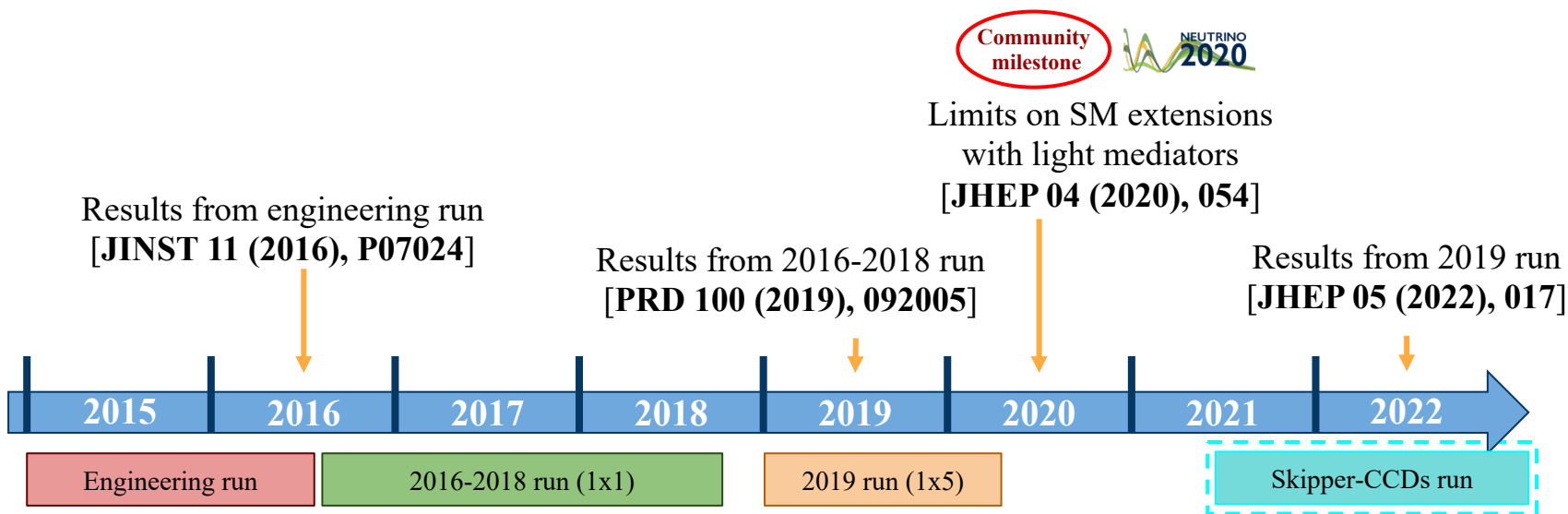
Lead – 15 cm
(gamma)

Outer Polyethylene – 30 cm
(neutrons)

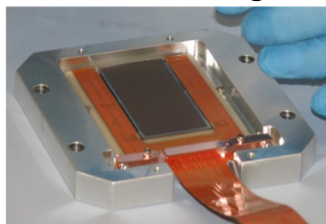




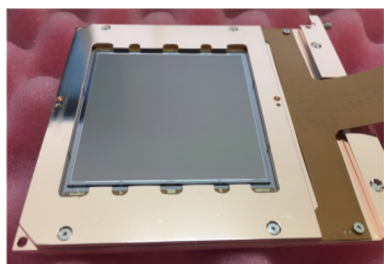
CONNIE experiment timeline



Installation at Angra



Installation of scientific CCDs



Installation of Skipper-CCDs

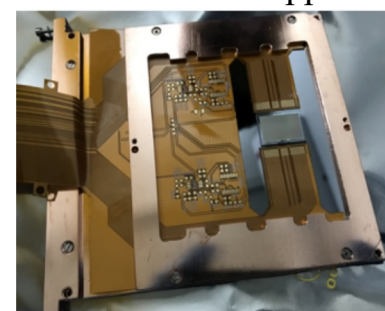


Image credit: Brenda Cervantes



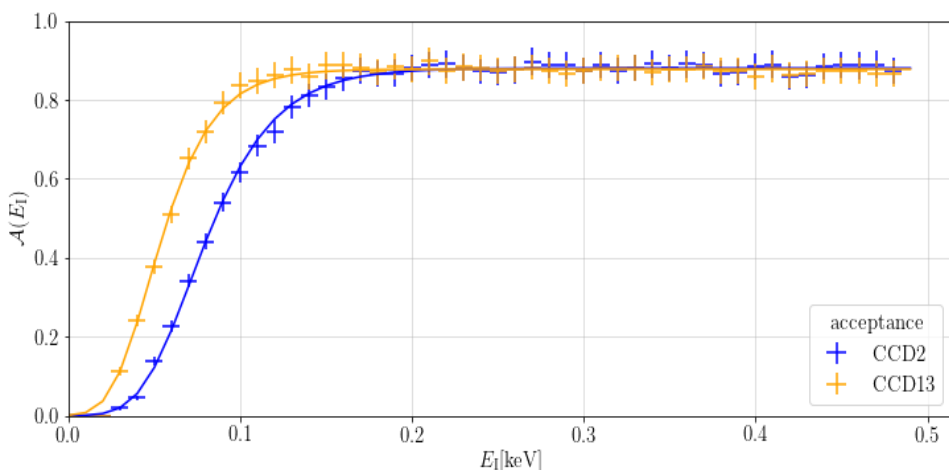
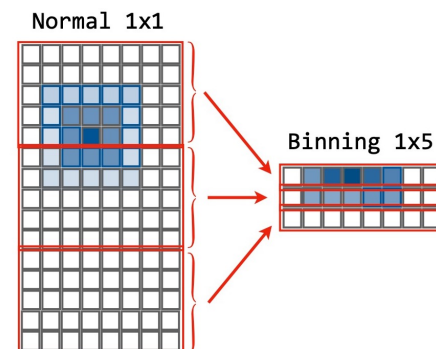
CONNIE 2019 run



Improvements in data acquisition and analysis techniques in 2019:

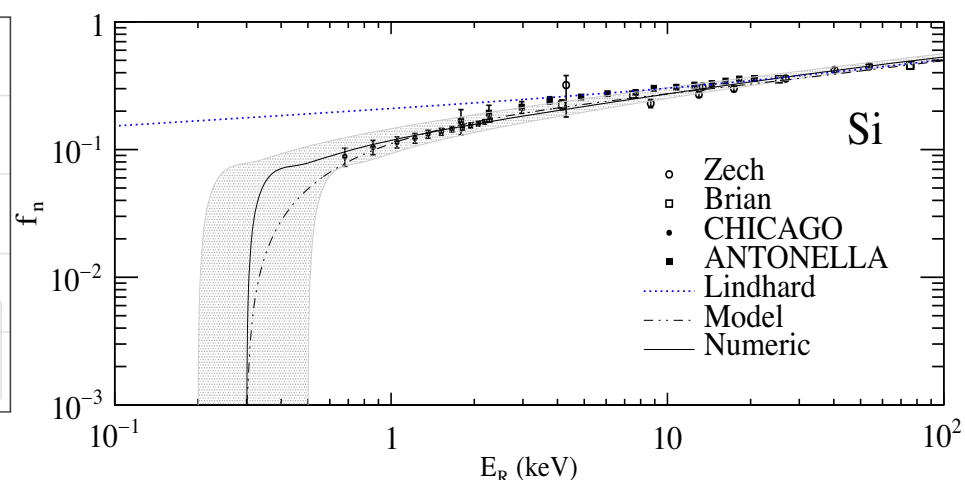
- 1x5 pixel hardware rebinning reduces readout noise.
- Improved energy and size-depth calibrations.
- Low-energy background characterisation and reduction.
 - Detection threshold is reduced to ~50 eV.
 - Full efficiency reached at 100-150 eV.
- Blind analysis and multiple cross-checks.
- New Sarkis quenching factor model for ionisation efficiency at low energies.

JHEP 05:017, 2022



Acceptance for most and least efficient CCDs

Y. Sarkis et al, PRD 101 (2020) 10 102001



Sarkis quenching factor model for Si

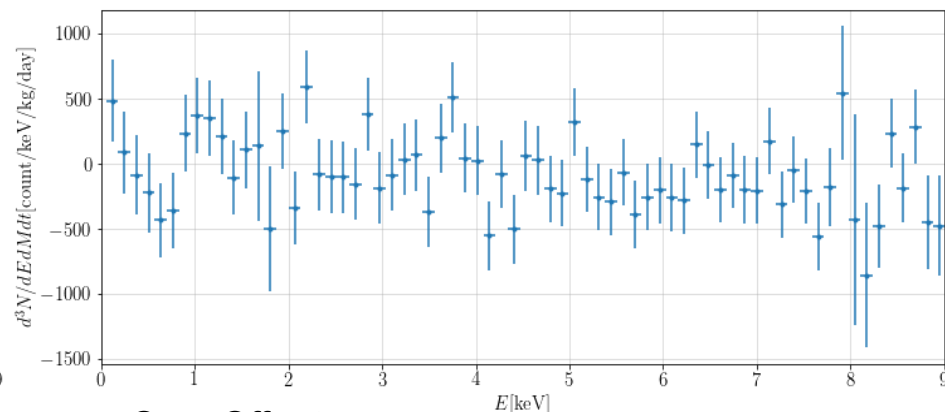
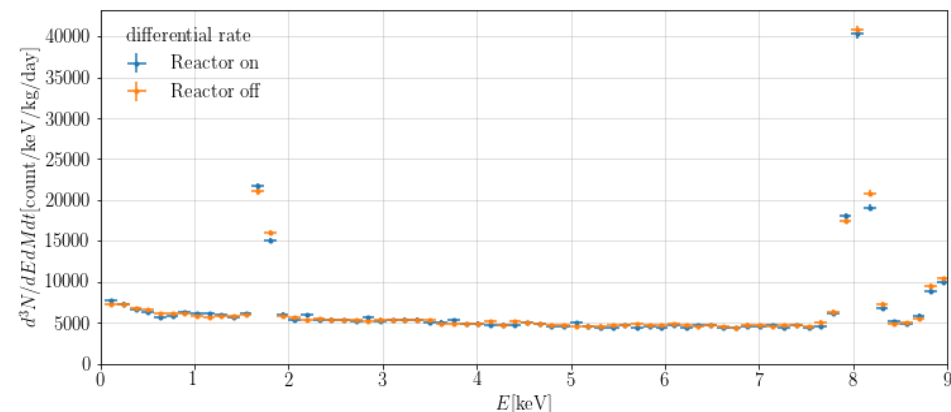


CONNIE 2019 results



JHEP 05:017, 2022

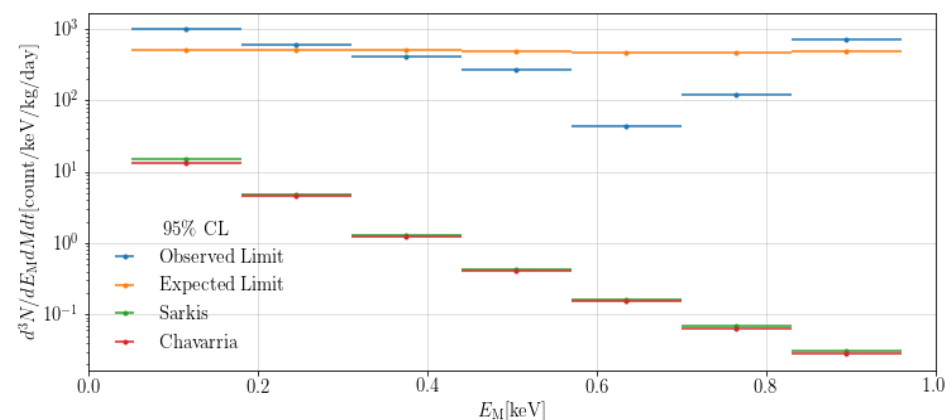
- Energy spectrum from 8 CCDs with total active fiducial mass 36 g.
- Exposures of 31.85 days with reactor on and 28.25 days with reactor off.
- Total exposure of 2.2 kg-days.



On - Off rates

Upper limits at 90% CL on the measured neutrino rate:

- Expected limit in the lowest-energy bin of (50-180) eV is 34-39 times the SM prediction.
- Observed limit is 66-75 times the prediction.



Preliminary
NEW

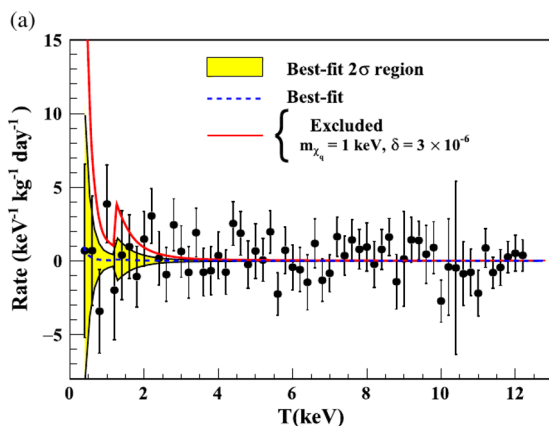
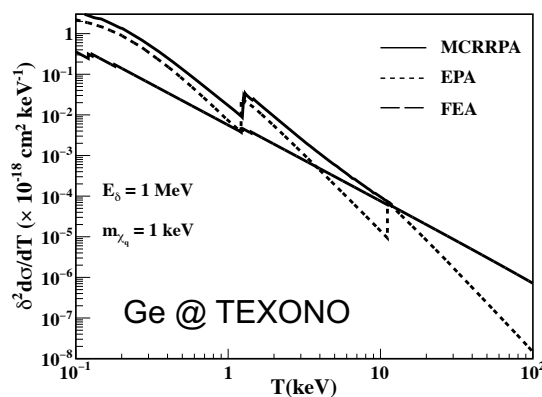
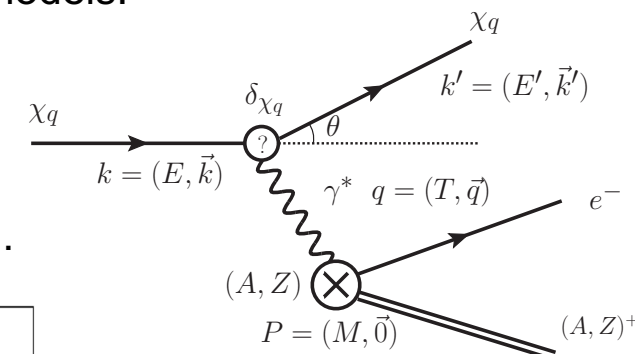
- The low-energy data can be used to search for relativistic millicharged particles (χ_q), predicted in hidden sector SM extensions.
- Can be pair-produced from Compton-like scattering of high-energy γ rays from reactors.
- Differential χ_q flux from the γ spectrum:

$$\frac{d\phi_{\chi_q}}{dE_{\chi_q}} = \frac{2}{4\pi R^2} \int \frac{1}{\sigma_{\text{tot}}} \frac{d\sigma}{dE_{\chi_q}} \frac{dN_\gamma}{dE_\gamma} dE_\gamma$$

- Interact with matter via atomic ionisation in t-channel.
- The interaction cross-section is calculated with different models.
- Expected differential count rates at the detector:

$$\frac{dR}{dT} = \rho_A \int_{E_{\text{min}}}^{E_{\text{max}}} \left[\frac{d\sigma}{dT} \right] \left[\frac{d\phi_{\chi_q}}{dE_{\chi_q}} \right] dE_{\chi_q}$$

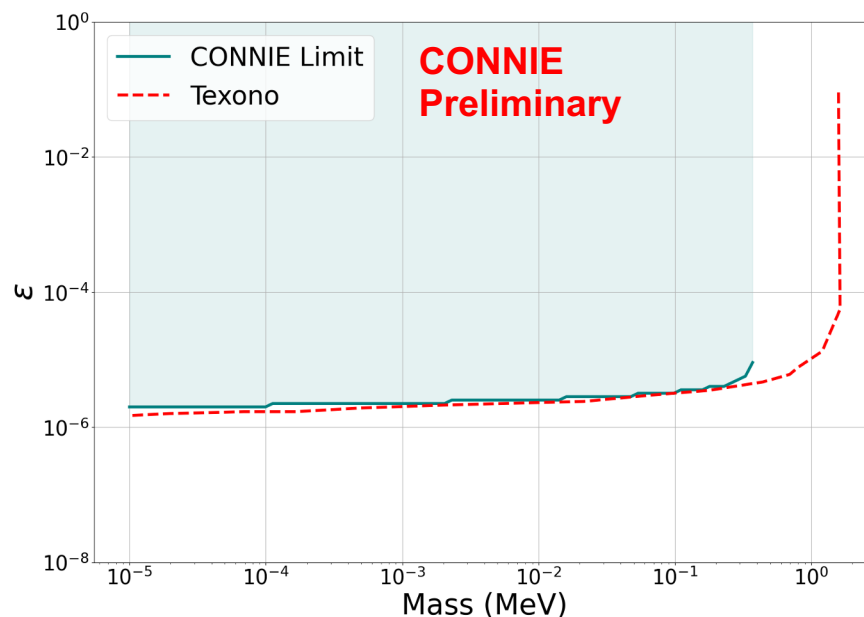
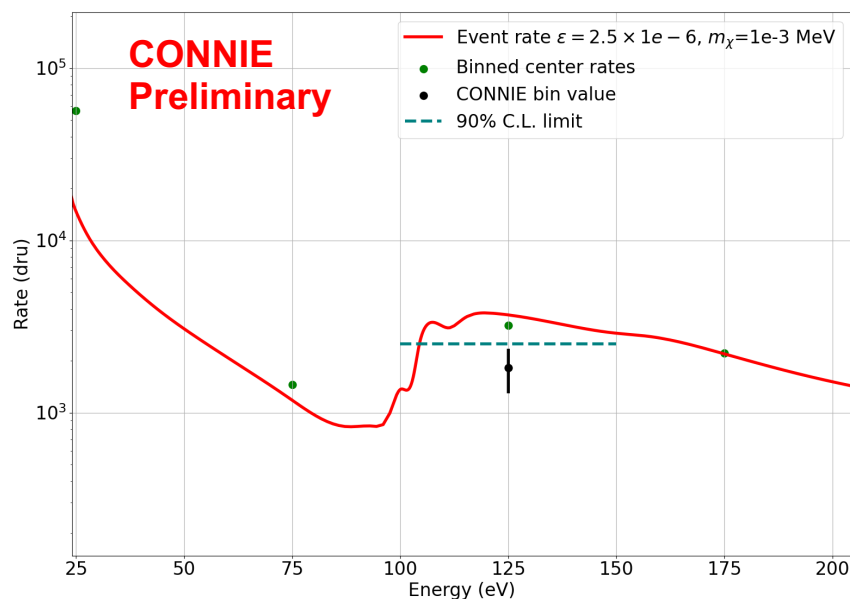
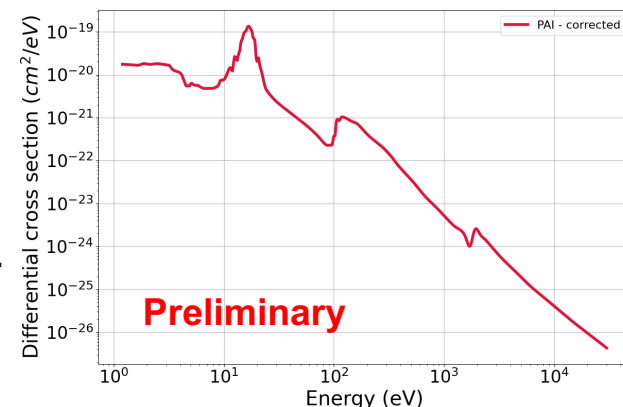
- On-off spectra can provide limits on reactor- χ_q production.



TEXONO collab., PRD 99, 032009 (2019)

Preliminary
NEW

- Interaction with silicon is modelled in the Photo Absorption Ionisation (PIA) model.
- Differential photo-absorption-ionisation cross-section for Si:
- Calculate the 90% CL on reactor- χ_q production for each mass and coupling using the (100-150) eV bin in 2019 data.
- Limit comparable to TEXONO, will update with full dataset.





CONNIE with skipper CCDs



- Skipper-CCD sensors offer a promising perspective to reach very low energies:

- Repeated non-destructive charge measurement.
- Reduction in electronic noise.
- Individual electron detection.

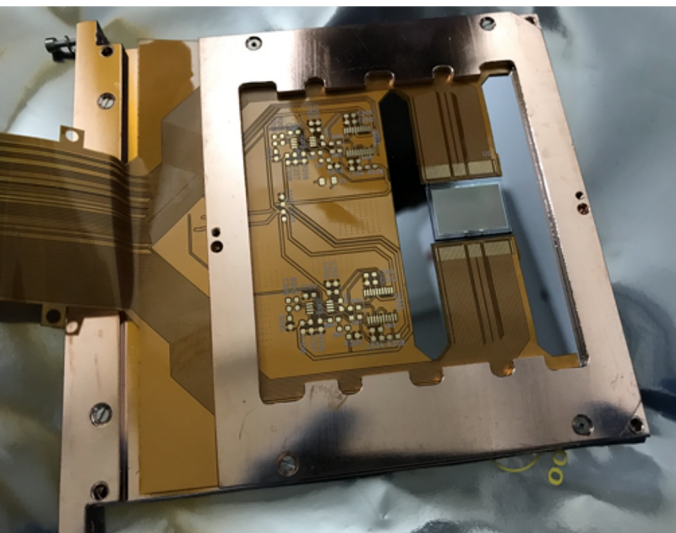
J. Tiffenberg et al, PRL 119 (2017)

See also E. Depaoli's talk
on Skipper-CCDs @Atucha

- Two skipper CCDs were installed at the CONNIE setup in July 2021.

- 0.5k x 1k pixels each, 675 μm thickness, 0.4 g total mass.
- New Low Threshold Acquisition readout electronics.
- New dedicated Vacuum Interface Board.

G. Cancelo et al, JATIS 7 (2021), 1 015001





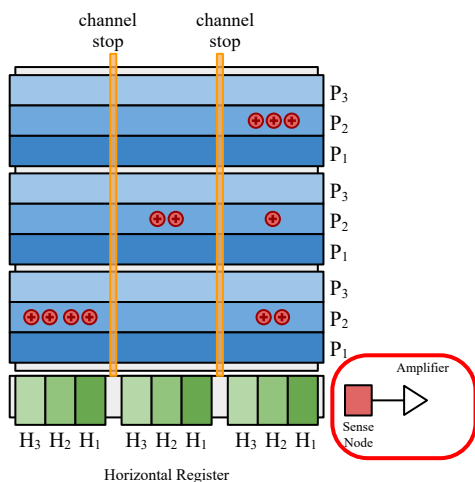
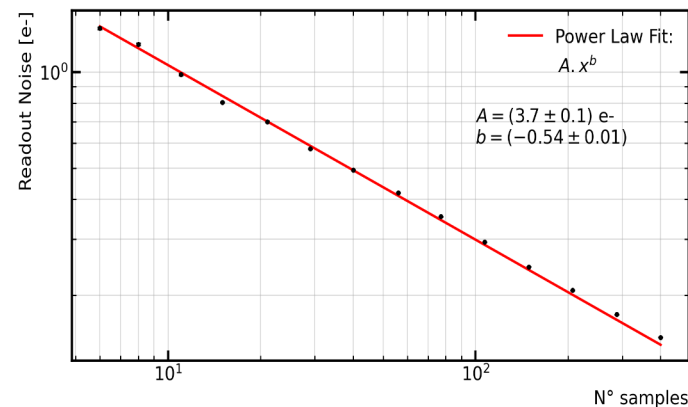
Skipper-CCD performance



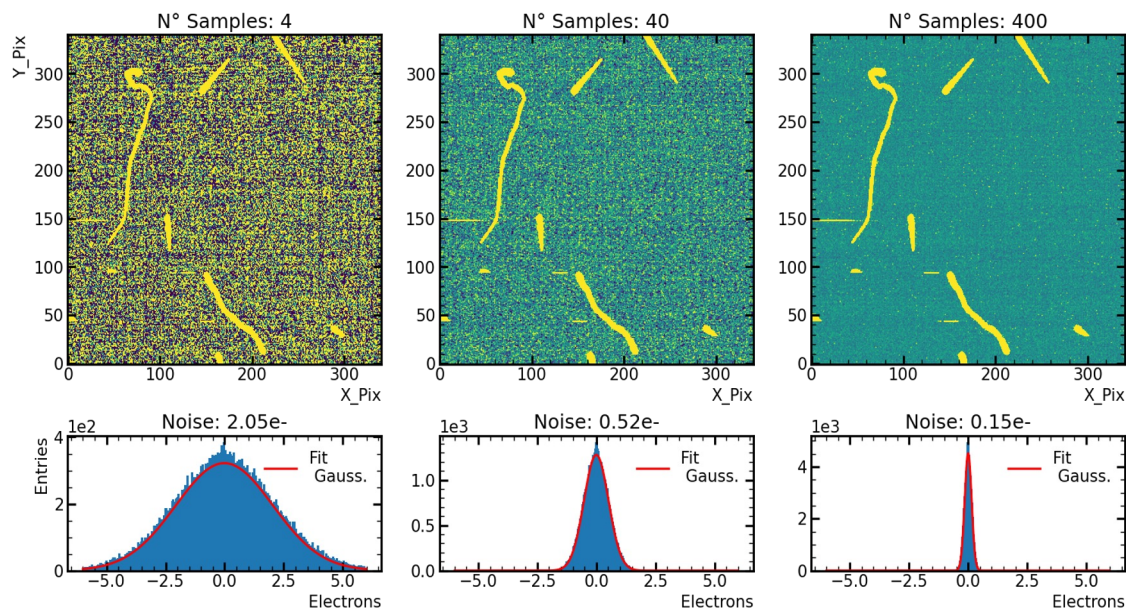
Preliminary

- Ongoing data taking to characterise skipper performance and background.
 - Tests of LTA acquisition and skipper readout mode.
 - Readout noise is reduced with N samples:

$$\sigma = \frac{\sigma_1}{\sqrt{N}}$$



Multiple non-destructive independent measurements of each pixel charge





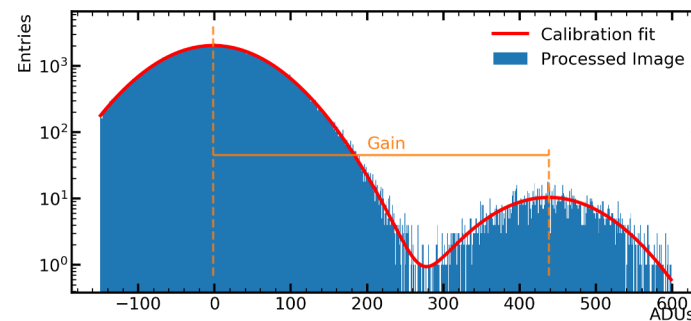
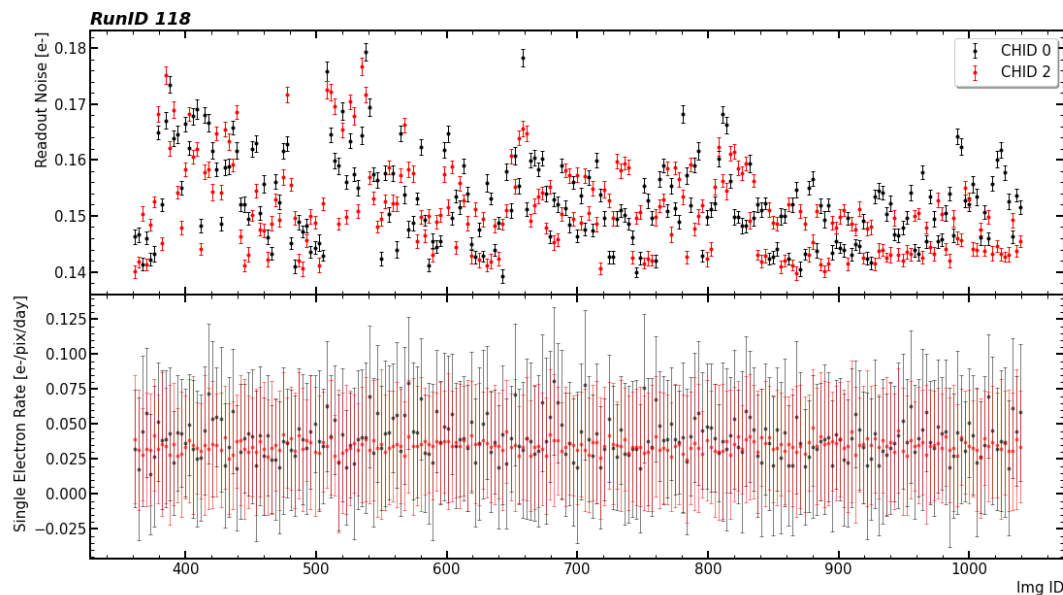
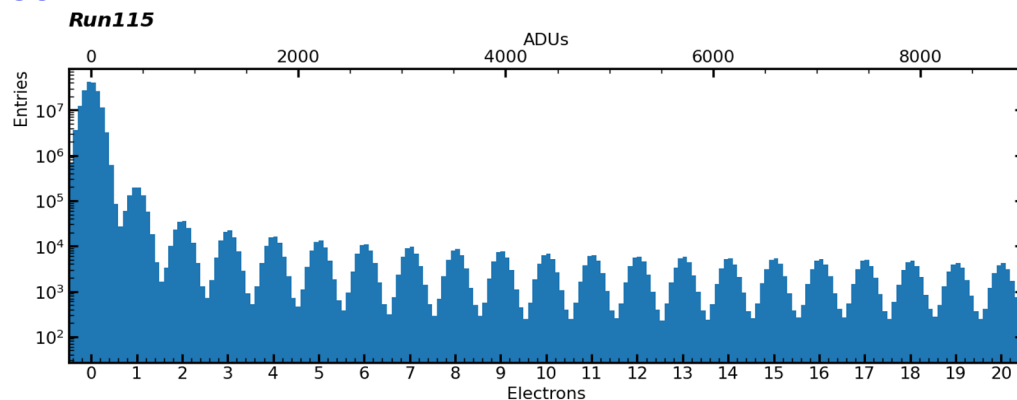
Skipper-CCD performance



Preliminary

Ongoing data taking to characterise skipper performance and background.

- Measurements of **dark current and noise**.
- **Energy calibration** and linearity.
- Event extraction and selection:
 - Masking hot columns/rows,
 - Excluding edges,
 - Excluding large-size events.



Preliminary:

Noise = 0.16 e-

Single-electron rate = 0.04 e-/pix/day



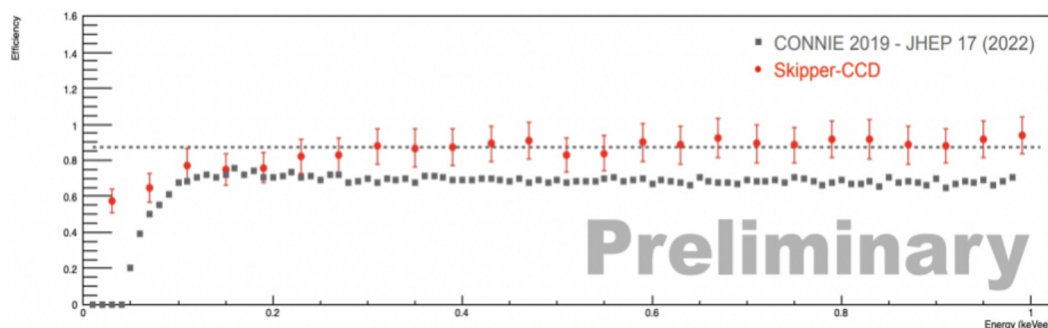
Skipper-CCD background



Preliminary

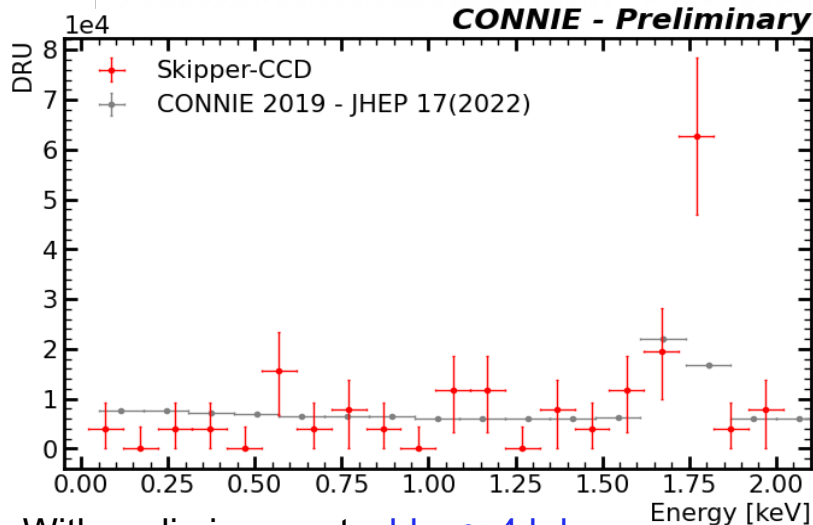
Ongoing data taking to characterise skipper performance and background.

- Efficiency determination.
- Background energy spectrum at sea level with passive shielding.
- Reactor-off data, a period of ~ 20 days. Total exposure 0.0028 kg-days .

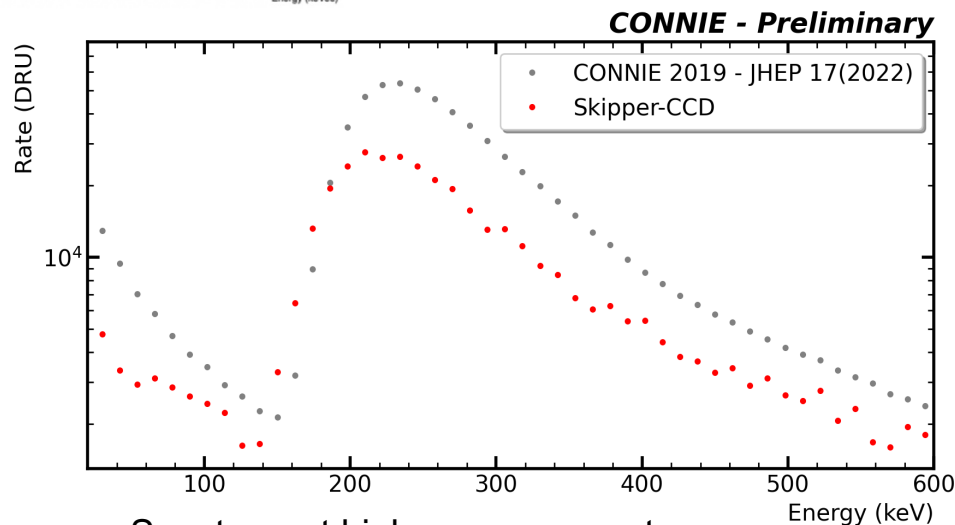


Efficiency

Threshold = 20 eV



With preliminary cuts: $\text{bkg} \cong 4 \text{ kdru}$



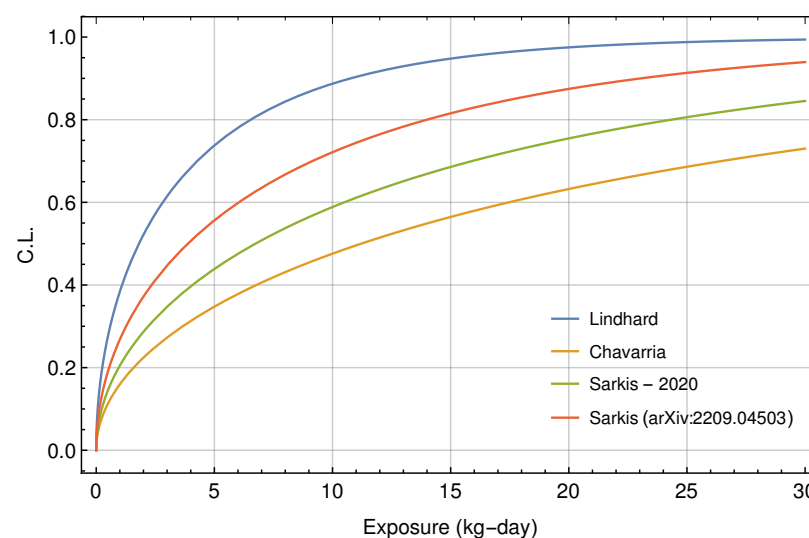
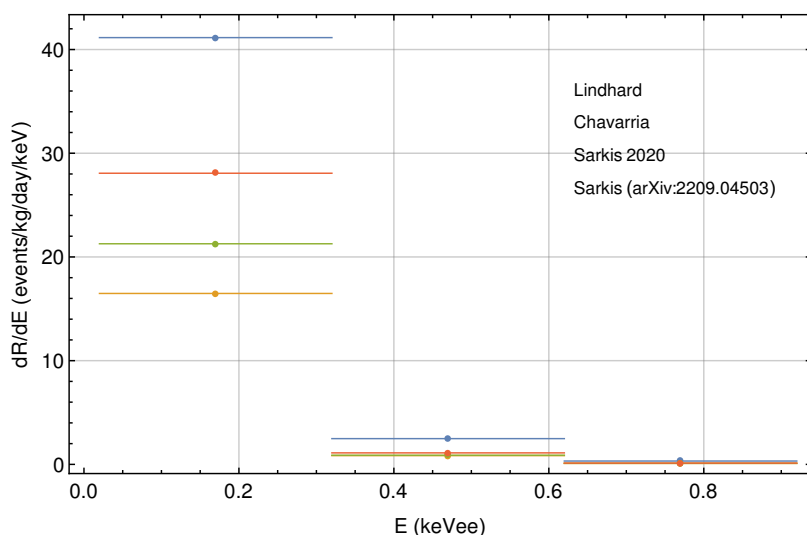
Spectrum at high energy, no cuts



CONNIE perspectives



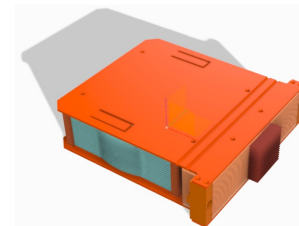
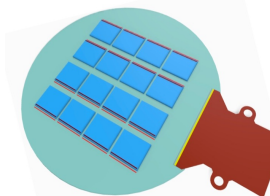
- Considering a threshold of 20 eV, we expect a **CEvNS rate 2.2 times higher** than in 2019.
- If we install a 1 kg detector at the CONNIE site, with a background rate 4 kdru, it should run for 11 (67) days if Lindhard (Chavarria) quenching factor to observe CEvNS at 90% CL.



- Studying the possibility to **increase sensor mass**.
 - New compact sensor arrangement.
 - New shielding design.
 - New vacuum interface board.
- Aim to go **closer at 20 m to the reactor**, below the dome.
 - Currently negotiating a position in Angra 2.

Multi-Chip Module
(16 CCDs \rightarrow 8 g)

Super Module
(16 MCMs \rightarrow 100 g)



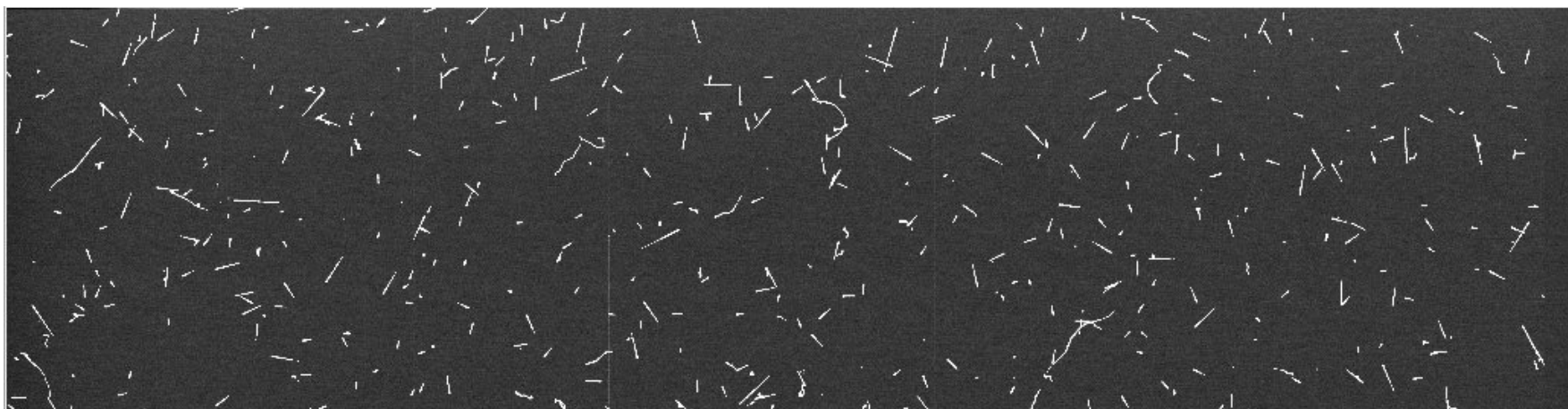
Oscura experiment design



Summary and outlook



- CCDs are a promising technology for detecting $\text{CE}\nu\text{NS}$ at low energies.
- Preliminary results using 2019 data show competitive limits on millicharged particles, will be updated with full dataset.
- CONNIE was the first experiment to install skipper CCDs at a reactor, in 2021.
- Excellent skipper-CCD performance with improved efficiency and background levels.
- Prospects to increase the sensor mass and move inside the Angra 2 reactor dome.





Back up





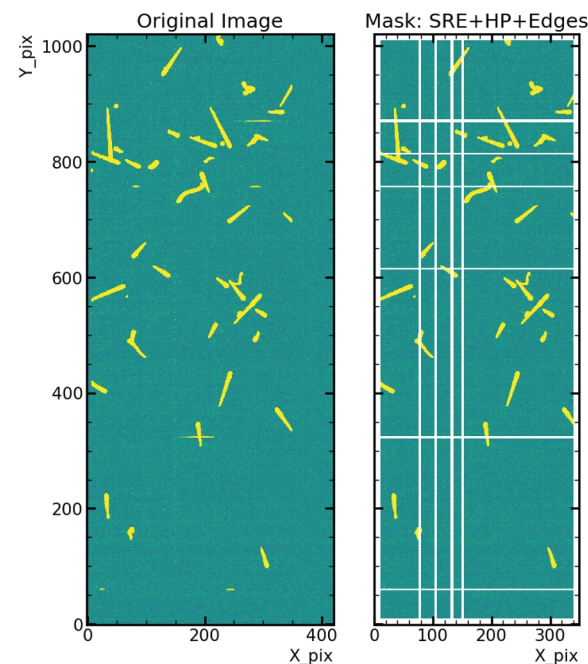
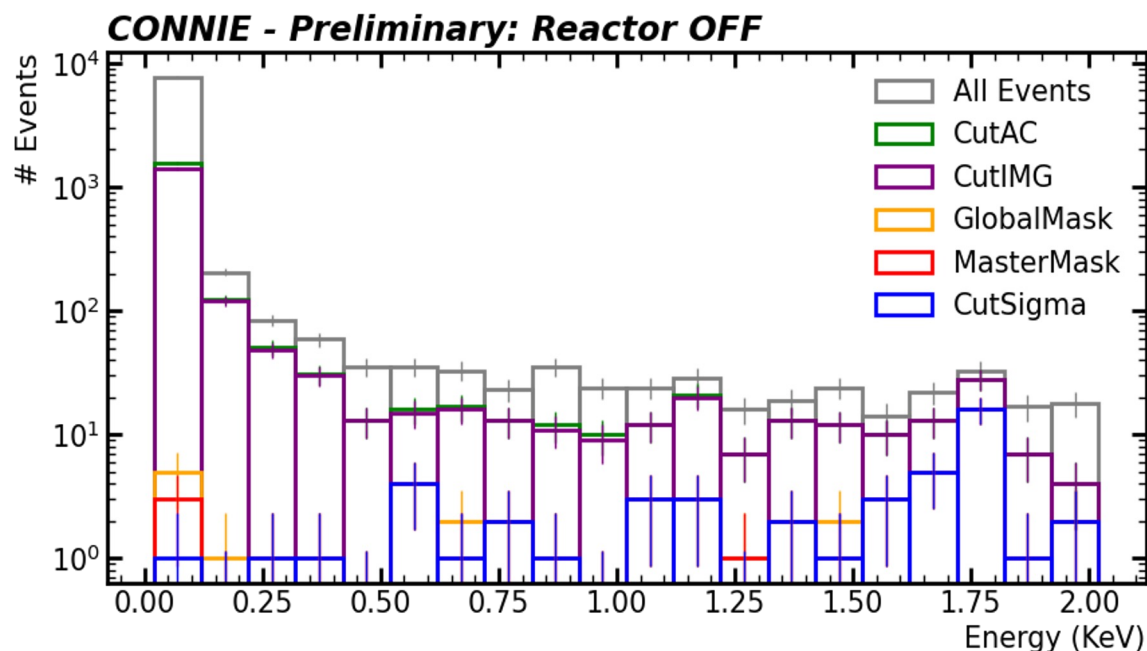
Skipper-CCD event selection



Preliminary

Selection cuts applied to reactor-off data:

- All Events: Energy threshold 20 eV;
- CutAC: 10 pixel border in the Active Region;
- CutIMG: Noise < 0.17 e- and SER < 0.14 e-/pix/day (Performance Cut);
- Mask: Global (Serial Register Event Mask + HotPixel Mask) + MasterHot;
- CutSigma: $X|Y\text{sigmaFit} < 1$ pixel.





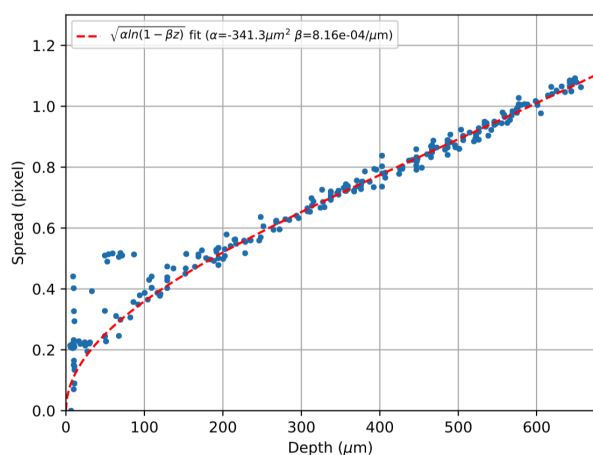
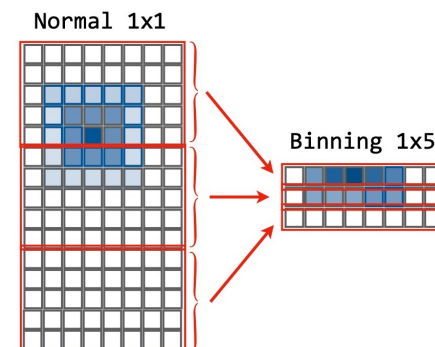
CONNIE 2019 run



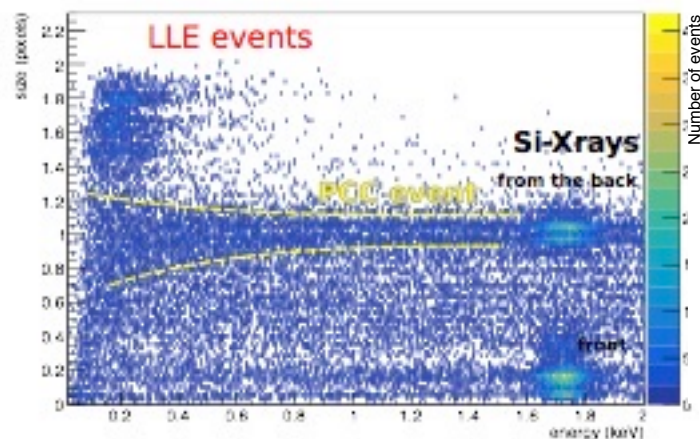
Improvements in data acquisition and analysis techniques in 2019:

JHEP 05:017, 2022

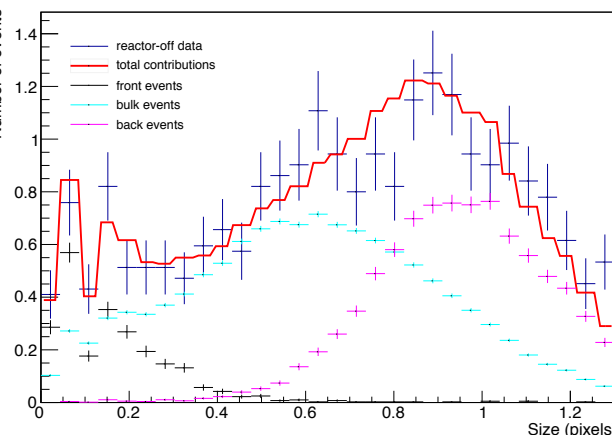
- 1x5 pixel hardware rebinning reduces readout noise.
- Improved energy and size-depth calibrations.
- Low-energy background characterisation and reduction:
 - Large low-energy events;
 - Partial-charge-collection layer.
- Blind analysis and multiple cross-checks.



Size-depth calibration from muons



Large-size low energy events from high-energy tails and inactive volume are excluded.



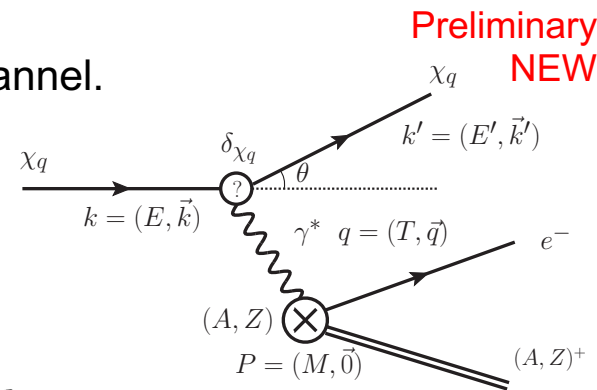
Partial-charge-collection layer at the back of the sensor

G. Fernandez-Moroni et al,
PRApplied 15 (2021), 6 064026

- Detection: interaction with silicon via atomic ionisation in t-channel.
- Photo Absorption Ionisation (PAI) semiclassical model.

$$\frac{d\sigma_R}{dE} = \underbrace{z^2 \frac{2k_R}{\beta^2} \left(\frac{1 - \beta^2 E/E_{max}}{E^2} \right)}_{ze \rightarrow ee}$$

$$\frac{d\sigma_{mcp}}{dE} = \epsilon^2 \frac{d\sigma_R}{dE} \longrightarrow \frac{d\sigma_{mcp}}{dE} = \epsilon^2 |F(E)|^2 \frac{d\sigma_R}{dE}$$



Modeling the Form Factor with the Photo Absorption Ionisation model:

Transverse		Longitudinal	
$\frac{d\sigma_{PAI}}{dE} = \underbrace{\frac{\alpha}{\beta^2 \pi} \frac{\sigma_\gamma(E)}{EZ} \ln[(1 - \beta^2 \epsilon_1)^2 + \beta^4 \epsilon_2^2]^{-1/2}}_{\text{Relativistic rise in e. deposition}} + \underbrace{\frac{\alpha}{\beta^2 \pi} \frac{1}{N_e \hbar c} \left(\beta^2 - \frac{\epsilon_1}{ \epsilon ^2} \right) \Theta}_{\text{Cherenkov}} + \underbrace{\frac{\alpha}{\beta^2 \pi} \frac{\sigma_\gamma(E)}{EZ} \ln\left(\frac{2mc^2 \beta^2}{E}\right)}_{\text{Resonance absorption at atomic energy levels}} + \underbrace{\frac{\alpha}{\beta^2 \pi} \frac{1}{E^2} \int_0^E \frac{\sigma_\gamma(E')}{Z} dE'}_{\text{Rutherford quasi free scatterings}}$			

$$\frac{d\sigma_{mcp}}{dE} = \epsilon^2 \frac{d\sigma_{PAI}}{dE}$$

Limit setting: we search for the lowest coupling compatible with what we observed in the 100-150 eV bin.

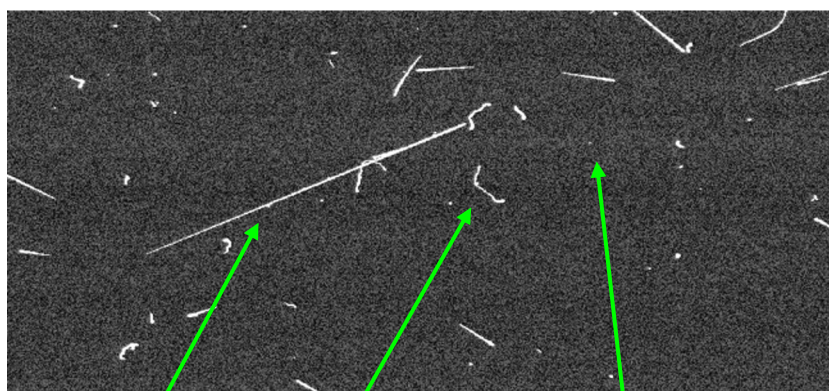


Event reconstruction



- Identify tracks based on geometry.
- Energy calibration in situ using Cu fluorescence x-rays.
- Depth versus diffusion width calibration using cosmic muons.
- Monitor the stability of natural backgrounds, noise and dark current.
- Low-energy neutrino selection based on likelihood test.

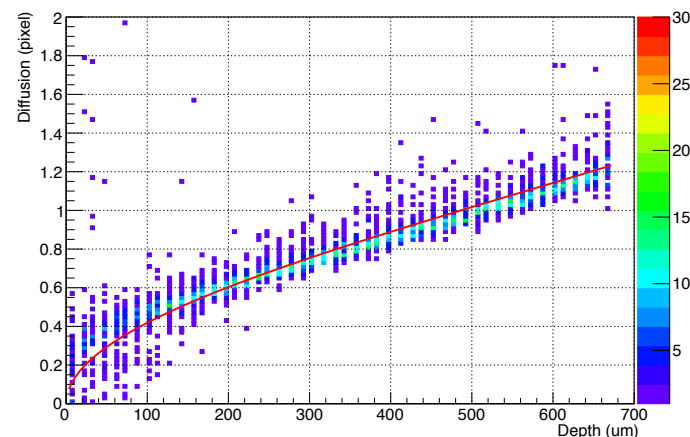
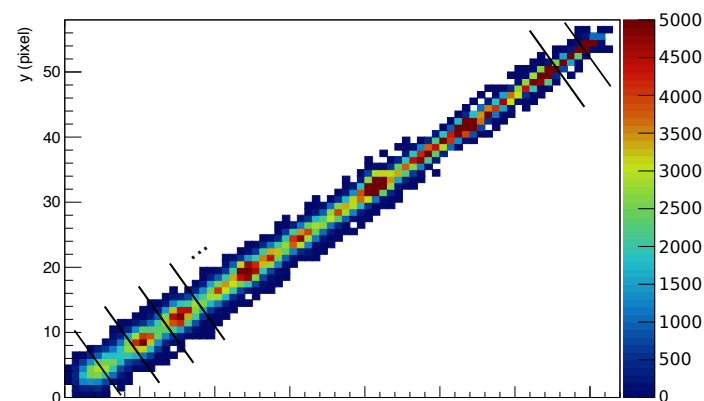
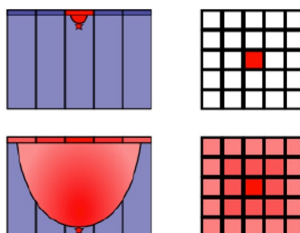
Phys. Rev. D 100 (2019) 092005



muon

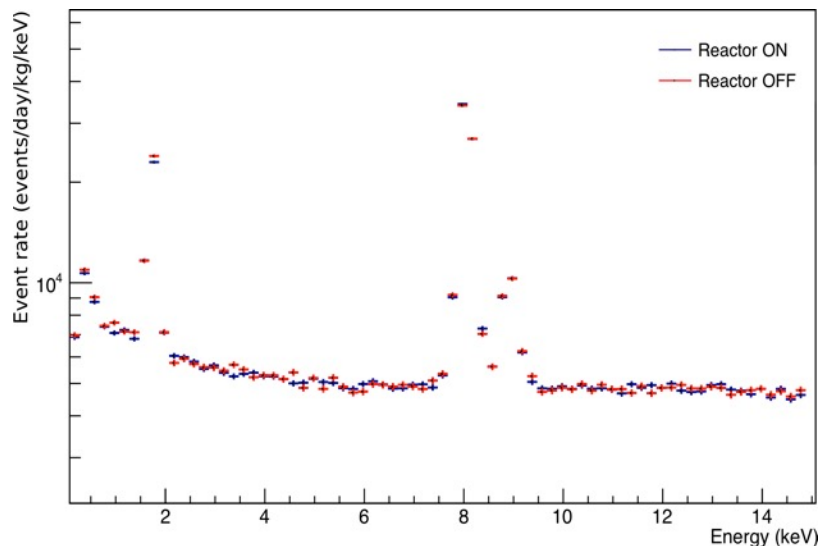
electron

diffusion-limited hits
photons/neutrinos



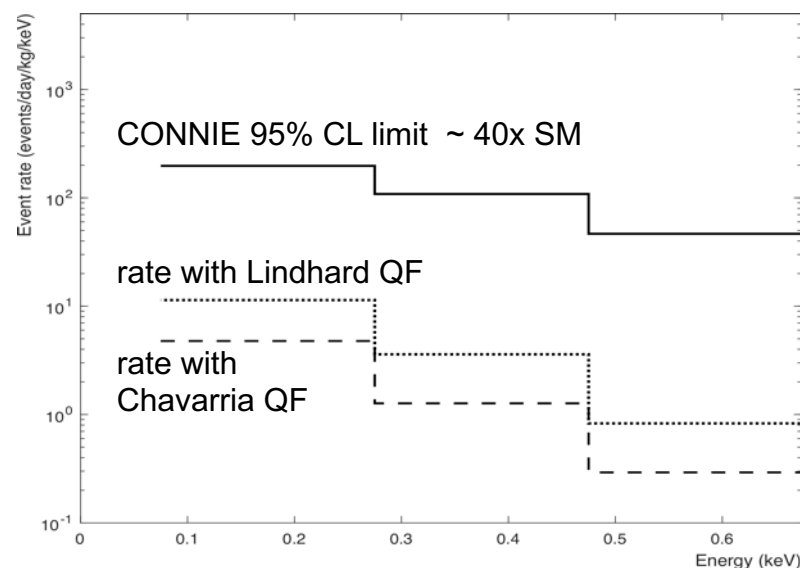
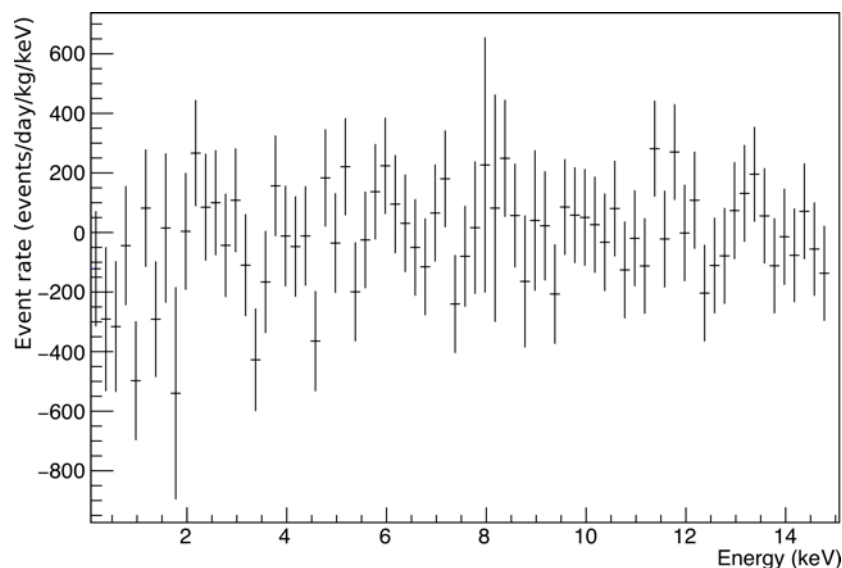


CONNIE Results 2016-18



Phys. Rev. D 100 (2019) 092005

- 2016-18 run with an active mass 47.6 g.
- Energy spectrum with **reactor on** (2.1 kg-day) vs **reactor off** data (1.6 kg-day).
- An **upper limit** is placed on CEvNS event rate, compared to expected rate depending on quenching factor.

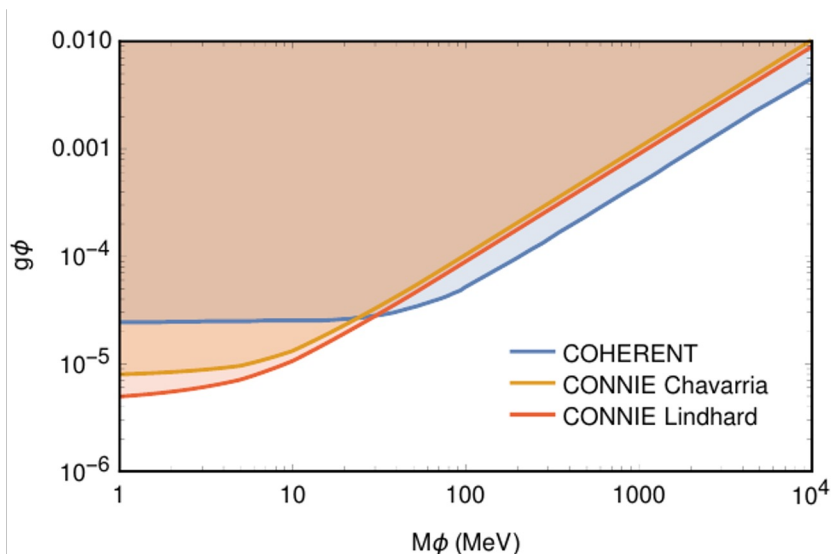




Non-standard interaction limits



JHEP 04 (2020) 054



- Event rates in the lowest-energy bin yield limits on non-standard neutrino interactions:
 - Light vector (Z') mediator.

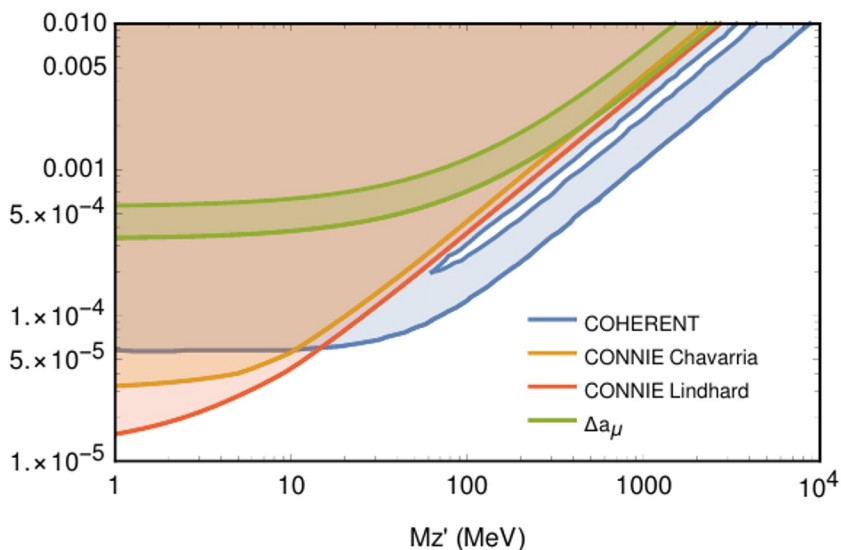
$$\frac{d\sigma_{SM+Z'}}{dE_R}(E_{\bar{\nu}_e}) = \left(1 - \frac{Q_{Z'}}{Q_W}\right)^2 \frac{d\sigma_{SM}}{dE_R}(E_{\bar{\nu}_e})$$

$$Q_{Z'} = \frac{3(N+Z)g'^2}{\sqrt{2}G_F(2ME_R + M_{Z'}^2)}.$$

- Light scalar (ϕ) mediator.

$$\frac{d\sigma_{SM+\phi}}{dE_R}(E_{\bar{\nu}_e}) = \frac{d\sigma_{SM}}{dE_R}(E_{\bar{\nu}_e}) + \frac{G_F^2}{4\pi} Q_\phi^2 \left(\frac{2ME_R}{E_{\bar{\nu}_e}^2}\right) MF^2(q)$$

$$Q_\phi = \frac{(14N+15.1Z)g_\phi^2}{\sqrt{2}G_F(2ME_R + M_\phi^2)}$$



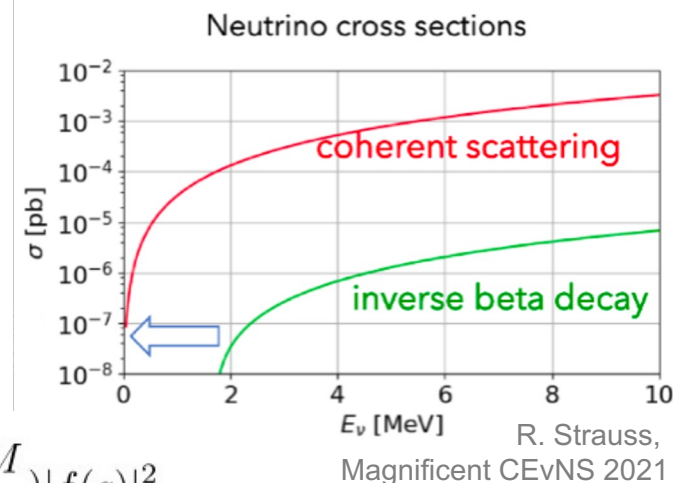
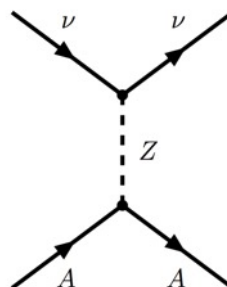
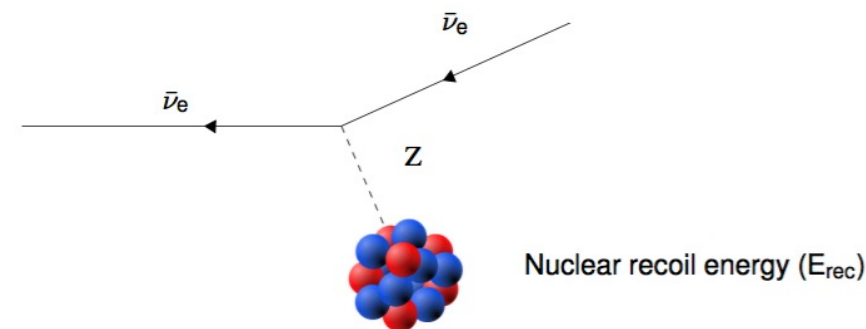
- We obtained the most stringent limits for low mediator masses $M_{Z'}(M_\phi) < 10$ MeV at the time.
- First competitive BSM constraints from CEvNS at reactors.



Coherent elastic νN scattering



- In the Coherent Elastic Neutrino-Nucleus Scattering (CEvNS) interaction, the neutrino scatters off the nucleus as a whole.
- Predicted in the Standard Model in 1974. D. Freedman, Phys.Rev. D 9 1389 (1974)
- Discovered by COHERENT in 2017 with neutrinos of $E_\nu \sim 20$ MeV with a CsI detector and later with a Liquid Ar detector. Science 357, 1123, 2017; PRL 129 8, 081801, 2022; PRL, 126, 012002, 2021



$$\frac{d\sigma}{dE_{\text{rec}}}(E_{\bar{\nu}_e}, E_{\text{rec}}) = \frac{G_F^2}{8\pi} [Z(4\sin^2\theta_W - 1) + N]^2 \times M \left(2 - \frac{E_{\text{rec}} M}{E_{\bar{\nu}_e}^2}\right) |f(q)|^2$$

- Coherent enhancement, nuclear form-factor is $f(q) \approx 1$ for low energies: $E_\nu < 50$ MeV.
- The total cross-section is $\approx 4.22 \times 10^{-45} N^2 E_\nu^2 \text{ cm}^2$ ($N = 14$ for Si).
- Reactor neutrinos with $E_\nu \sim 1$ MeV can probe new physics at low energies.

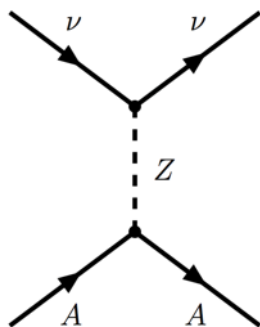


New Physics with neutrinos

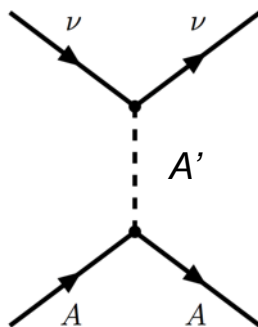


- The coherent scattering rates are calculated with precision in the SM.
- Any discrepancy can be a sign of contributions from “New Physics” interactions:
 - Non-standard interactions of neutrinos.
 - Light sterile neutrinos.
 - Neutrino magnetic moment.
 - Neutrino millicharge.

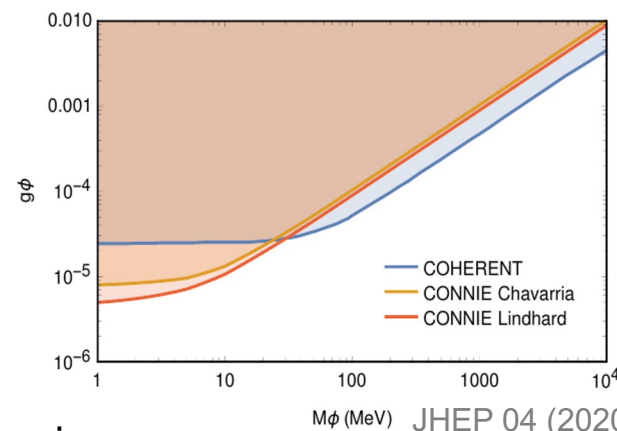
Standard Model



Model with New Physics



Y. Farzan et al, JHEP 05 (2018) 066
D.K. Papoulias et al, Front. Phys. 7 (2019) 191
J. Dent et al, PRD 96 (2017) 095007
T. Kosmas et al, PRD 96 (2017) 063013
O. Miranda et al, JHEP 07 (2019) 103
O. Parada, Adv. HEP 2020 (2020) 5908904



- Also important for direct DM searches and supernova physics.
- Weak angle measurement.
- Once the detection is established, it can be used to create compact detectors for reactor monitoring.

B. Cañas et al, PLB 784 (2018) 159
G. Fernandez-Moroni et al, JHEP 03 (2021) 186
B. Cogswell, P. Huber, Science and Global Security 24, 2 (2016) 114